Supporting Information

The synthesis, characterization and application of the binol-cages of R-/S-enantiomers

Tianyu Li, Luyao Ding, Yihong Kang, Xin-Qi Hao, Yujing Guo*, Linlin Shi*, Mao-Ping Song

College of Chemistry, Zhengzhou University, Zhengzhou 450001, Henan, China.

***Correspondence to:** Prof. Linlin Shi, College of Chemistry, Zhengzhou University, No.100 Science Avenue, Zhengzhou 450001, Henan, China. E-mail: linlinshi@zzu.edu.cn; Prof. Yujing Guo, College of Chemistry, Zhengzhou University, No.100 Science Avenue, Zhengzhou 450001, Henan, China. E-mail: yujingguo@zzu.edu.cn

1. Materials and Methods

All reagents were purchased from Sigma-Aldrich, Shanghai, China, Fisher, Shanghai, China, Across, Shanghai, China, and Alfa Aesar, Tianjin, China, and they were used without further purification. Tetrahydrofuran (THF) was dried over sodium metal and freshly distilled under nitrogen atmosphere prior to use. All air-sensitive reactions were carried out under inert N_2 atmosphere. Column chromatography was conducted using SiO_2 (VWR, 40-60 μm, 60 Å) and the separated products were visualized by UV light. NMR spectra data were recorded on a 600 MHz Bruker NMR spectrometer in $CDCl_3$ with TMS as the reference. Emission spectra in the liquid state were recorded on a Horiba-FluoroMax-4 spectrofluorometer, HORIBA, Edison, NJ, USA. Circular dichroism (CD) spectra were recorded on Applied Photophysics Chirascan circular dichroism chiroptical spectrometer at room temperature. After adding solution of chiral cages in $CHCl_3$ (c = 0.1 mM) to the sample cell (l = 0.5 mm), the CD data were then recorded in a wavelength range of 240−400 nm. ESI-MS of cages was recorded with a Waters Synapt G2-Si mass spectrometer, USA and the experiments were performed with a Waters Q-Tof Micro MS/MS high-resolution mass, USA, spectrometer in ESI mode.The instrument used in the mass spectrometry experiment of compound **7** is Agilent 1290/InfinityII6546, Singapore. The data is recorded by Qualitative Analysis 10.0. The Fourier Transform Infrared FT-IR spectra were recorded on a Spectrum TWO FT-IR spectrophotometer, PerkinElmer, Llantrisant, UK. All heating reactions were completed in a metal bath.

2.Synthesis of chiral BINOL cages

2.1 Synthesis of compound 2[1]

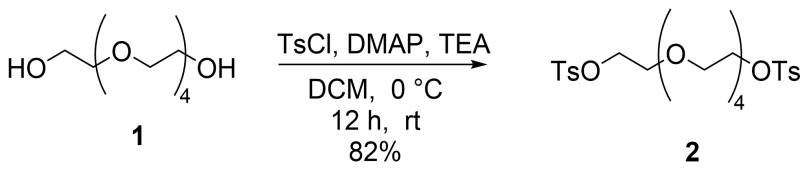

Pentaethylene glycol (276.6 mg, 2 mmol) was added to 52 mL of dichloromethane, stirred at 0 ºC for 5 min, then DMAP (50 mg, 0.41 mmol) and TsCl (762.6 mg, 4

mmol) were added, and triethylamine (0.84 ml) was added dropwise in the solution. The reaction mixture was stirred at the same temperature for 2 h, and then stirred at room temperature for 12 h. After complete consumption of the starting material. The mixture was concentrated in vacuo. The residue was purified by column chromatography over silica gel (petroleum ether: ethyl acetate = 2: 1) to afford **2** as a colorless oil.

Compound **2** (895.7 mg, 82% yield) ^{1}H NMR (600 MHz, Chloroform-*d*) δ (ppm)7.83 – 7.77 (m, 4H), 7.34 (d, J = 8.0 Hz, 4H), 4.19 – 4.12 (m, 4H), 3.71 – 3.67 (m, 4H), 3.60 (s, 4H), 3.58 (s, 8H), 2.44 (s, 6H). ^{13}C NMR (151 MHz, Chloroform-*d*) δ (ppm) 144.81, 129.83, 127.95, 70.73, 70.58, 70.49, 69.27, 68.66, 21.63.

2.2 Synthesis of (*S*)- and (*R*)-4[2]

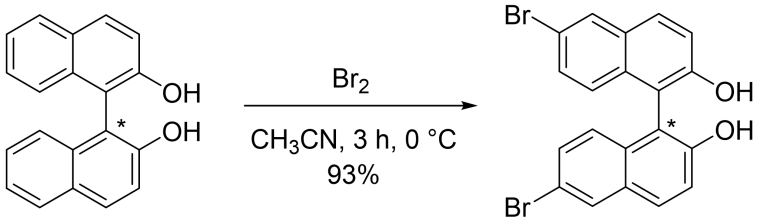

(*S*) -or (*R*)-3 **(*S*)- or (*R*)- 4**

(*S*)- or **(*R*)-3** (1 g, 0.003 mmol) was added to 17.48 mL of acetonitrile. Bromine (0.54 mL 0.01 mmol) was added to the solution slowly. The reaction mixture was stirred at 0 °C temperature for 3 hours. The reaction was then quenched and washed with saturated sodium bisulfite solution to remove unreacted bromine. The reaction mixture was extracted by CH2Cl2 and washed with water and brine. The organic layer was dried over Na2SO4, concentrated in vacuo afford the product as brown solid.

(*S*)-4 (1.43 g, 92% yield) ^{1}H NMR (600 MHz, Chloroform-*d*) δ (ppm) 8.05 (d, J = 2.0 Hz, 2H), 7.89 (d, J = 9.0 Hz, 2H), 7.41 – 7.35 (m, 4H), 6.96 (d, J = 9.0 Hz, 2H), 5.03

(s, 2H). ^{13}C NMR (151 MHz, Chloroform-*d*) δ (ppm) 152.98, 131.90, 130.86, 130.68, 130.58, 130.45, 125.88, 118.99, 118.02, 110.69.

(*R*)-4 (1.44 g, 93% yield) ^{1}H NMR (600 MHz, Chloroform-*d*) δ (ppm) 8.05 (d, J = 2.0 Hz, 2H), 7.89 (d, J = 9.0 Hz, 2H), 7.41 – 7.36 (m, 4H), 6.96 (d, J = 8.9 Hz, 2H), 5.04 (s, 2H). ^{13}C NMR (151 MHz, Chloroform-*d*) δ (ppm) 152.99, 131.89, 130.87, 130.70, 130.59, 130.45, 125.88, 118.98, 118.02, 110.67.

2.3 Synthesis of (*S*)- and (*R*)-5[3]

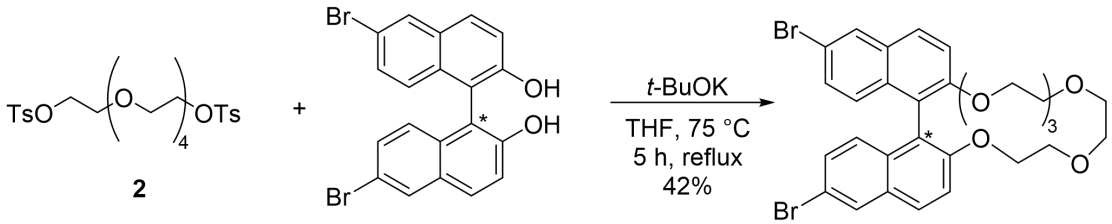

t-BuOK (224.7 mg, 2 mmol) were added to 40 mL of the THF solution containing **4** (444 mg, 1 mmol) under argon atmosphere. Then compound **2** (546 mg, 1 mmol) was added to the reaction mixture and reflux at 75 °C for 5 h. Upon completion of reaction, the solvent was removed in vacuum, and the residue was added to 100 mL of $CH2Cl_2$ and washed by water. The organic layer was dried over Na_2SO4, concentrated and purified by silica column chromatography (CH_2CL_2: CH_3OH = 200:1,v:v) to afford the product **(*R*)-** or **(*S*)-5** as white powder.

(*R*)-5 (270 mg, 42% yield) ^{1}H NMR (600 MHz, Chloroform-*d*) δ (ppm) 8.01 (d, J = 2.0 Hz, 2H), 7.85 (d, J = 9.0 Hz, 2H), 7.48 (d, J = 9.0 Hz, 2H), 7.28 – 7.26 (m, 2H), 6.95 (d, J = 9.0 Hz, 2H), 4.19 (ddd, J = 10.9, 7.2, 3.9 Hz, 2H), 4.05 – 4.02 (m, 2H), 3.64 – 3.60 (m, 4H), 3.55 – 3.49 (m, 8H), 3.30 – 3.34 (m, 4H). ^{13}C NMR (151 MHz, Chloroform-*d*) δ (ppm) 154.76, 132.47, 130.41, 129.81, 129.64, 128.53, 127.09, 120.03, 117.51, 116.89, 70.86, 70.66, 70.62, 69.79, 69.76.

(*S*)-5 (257 mg, 40% yield) ^{1}H NMR (600 MHz, Chloroform-*d*) δ (ppm) 8.00 (d, J = 2.0 Hz, 2H), 7.84 (d, J = 9.0 Hz, 2H), 7.48 (d, J = 9.0 Hz, 2H), 7.27 – 7.26 (m, 2H), 6.95 (d, J = 9.0 Hz, 2H), 4.19 (ddd, J = 10.9, 7.2, 3.9 Hz, 2H), 4.05 – 4.01 (m, 2H), 3.64 – 3.60 (m, 4H), 3.55 – 3.48 (m, 8H), 3.40 – 3.34 (m, 4H). ^{13}C NMR (151 MHz, Chloroform-*d*) δ (ppm) 154.76, 132.47, 130.41, 129.81, 129.64, 128.53, 127.10, 120.03, 117.51, 116.89, 70.86, 70.66, 70.62, 69.79, 69.76.

2.4 Synthesis of (*S*)- and (*R*)-7

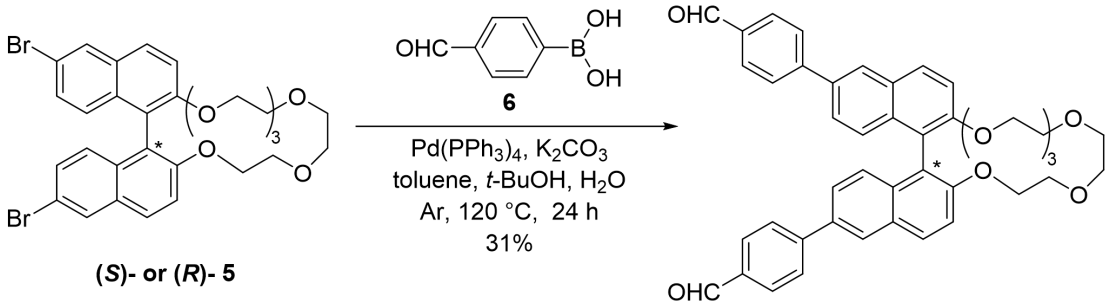

(*S*)- or (*R*)- 5

(*S*)- or (*R*)- 7

After **(*S*)-** or **(*R*)-5** (367 mg, 0.569 mmol), 4-formylphenylboronic acid (342 mg, 2.28 mmol), $Pd(PPh_3)_4$ (111.94 mg, 0.093 mmol), K_2CO_3 (787.57 mg, 5.7 mmol) were added to a flask, a mixture of toluene, *t*-BuOH and H_2O (3:1:1, V:V:V) was added under argon atmosphere. The reaction mixture was stirred at 120 °C for 24 h. Upon completion of reaction, the solvent was removed in vacuum, and the residue was added to 100 mL of CH_2Cl_2 and washed by water. The organic layer was dried over Na_2SO_4, concentrated and purified by silica column chromatography (CH_2CL_2:CH_3OH = 200:1, v:v) to afford the product **5** as pale yellow solid.

(*S*)-7 (118.81 mg, 30% yield) ^{1}H NMR (600 MHz, Chloroform-*d*) δ (ppm) 10.06 (s, 2H), 8.16 (d, J = 1.9 Hz, 2H), 8.05 (d, J = 9.0 Hz, 2H), 7.98 – 7.96 (m, 4H), 7.86 – 7.83 (m, 4H), 7.57 – 7.52 (m, 4H), 7.27 (s, 2H), 4.28 – 4.24 (m, 2H), 4.13 – 4.10 (m, 2H), 3.68 – 3.63 (m, 4H), 3.58 – 3.51 (m, 8H), 3.43 (t, J = 4.4 Hz, 4H). ^{13}C NMR (151 MHz, Chloroform-*d*) δ (ppm) 191.87, 155.24, 147.11, 135.03, 134.74, 133.86,

130.34, 129.99, 129.46, 127.61, 126.67, 126.29, 125.55, 120.09, 116.63, 70.91, 70.69, 70.63, 69.80.

(*R*)-7 (122.77 mg, 31% yield) ^{1}H NMR (600 MHz, Chloroform-*d*) δ (ppm) 10.06 (s, 2H), 8.16 (d, J = 1.9 Hz, 2H), 8.05 (d, J = 9.0 Hz, 2H), 8.00 – 7.94 (m, 4H), 7.90 – 7.82 (m, 4H), 7.60 – 7.50 (m, 4H), 7.27 (s, 2H), 4.28 – 4.24 (m, 2H), 4.13 – 4.10 (m, 2H), 3.64 (d, J = 9.6 Hz, 4H), 3.59 – 3.51 (m, 8H), 3.44 (d, J = 5.1 Hz, 4H). ^{13}C NMR (151 MHz, Chloroform-*d*) δ (ppm) 191.87, 155.23, 147.11, 135.02, 134.73, 133.86, 130.34, 129.99, 129.46, 127.61, 126.67, 126.29, 125.55, 120.08, 116.63, 70.91, 70.69, 70.63, 69.80.

2.5 Synthesis of (*S*)- and (*R*)-8[4]

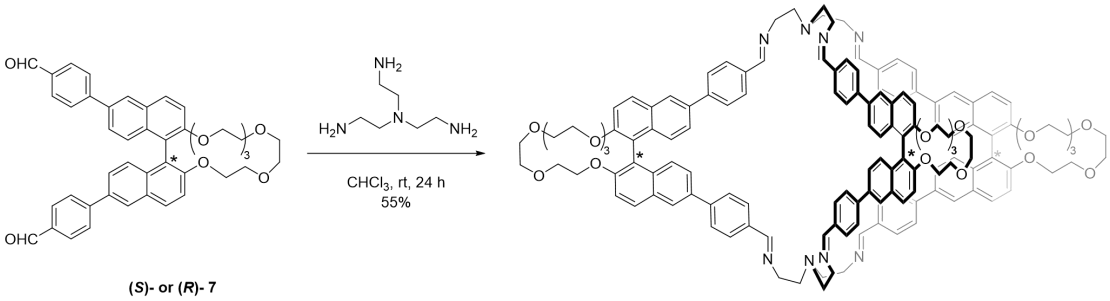

A solution of tris(2-aminoethyl)amine (373 μL, 0.086 mmol, 0.2 M in chloroform) was added dropwise into a solution of **(*S*)-** or **(*R*)-7** (71 mg, 0.1mmol) in 20 mL of chloroform. After the reaction mixture was stirred at 25 °C for 24 h, the mixture was poured into 50 mL of methanol. The precipitate was filtered and dried under vacuum to afford **(*S*)-** or **(*R*)-8** as a white solid.

(*S*)-8 (42.45 mg, 55% yield) ^{1}H NMR (600 MHz, Chloroform-*d*) δ (ppm) 8.01 (s, 6H), 7.95 (d, J = 8.9 Hz, 6H), 7.63 (s, 6H), 7.43 (dd, J = 8.5, 6.4 Hz, 18H), 7.33 (dd, J = 8.6, 1.9 Hz, 6H), 7.27 (d, J = 8.7 Hz, 6H), 6.99 (d, J = 7.8 Hz, 12H), 4.14 – 4.09 (m, 6H), 3.94 (dt, J = 10.8, 4.3 Hz, 6H), 3.63 – 3.59 (m, 12H), 3.54 – 3.52 (m, 16H), 3.48 (q, J = 4.1 Hz, 12H), 3.41 – 3.37 (m, 8H), 3.31 (t, J = 4.3 Hz, 12H), 2.96 – 2.91 (m, 6H), 2.80 (dd, J = 13.2, 6.2 Hz, 6H). ^{13}C NMR (151 MHz, Chloroform-*d*) δ (ppm)

161.14, 154.70, 144.12, 136.47, 135.03, 133.42, 129.52, 129.49, 128.67, 127.84, 126.17, 125.72, 120.25, 116.57, 70.82, 70.66, 70.58, 69.77, 69.70, 59.95, 56.71.

(*R*)-8 (41 mg, 53% yield) ^{1}H NMR (600 MHz, Chloroform-*d*) δ (ppm) 8.01 (s, 6H), 7.95 (d, J = 8.9 Hz, 6H), 7.63 (s, 6H), 7.43 (t, J = 7.9 Hz, 18H), 7.32 (d, J = 8.6 Hz, 6H), 7.28 (d, J = 8.7 Hz, 6H), 6.99 (d, J = 7.7 Hz, 12H), 4.13 -4.10 (m, 6H), 3.94 (dt, J = 10.0, 4.3 Hz, 6H), 3.61 -3.59 (m, 12H), 3.55 – 3.52 (m, 16H), 3.48 (q, J = 4.0 Hz, 12H), 3.41 -3.37 (m, 8H), 3.31 (t, J = 4.3 Hz, 12H), 2.93 (t, J = 11.0 Hz, 6H), 2.80 (dd, J = 13.6, 6.2 Hz, 6H). ^{13}C NMR (151 MHz, Chloroform-*d*) δ (ppm) 161.14, 154.70, 144.12, 136.47, 135.03, 133.42, 129.52, 129.49, 128.67, 127.84, 126.17, 125.72, 120.25, 116.57, 70.82, 70.66, 70.58, 69.77, 69.70, 59.95, 56.71.

2.6 NMR and ESI-MS spectra of the compounds

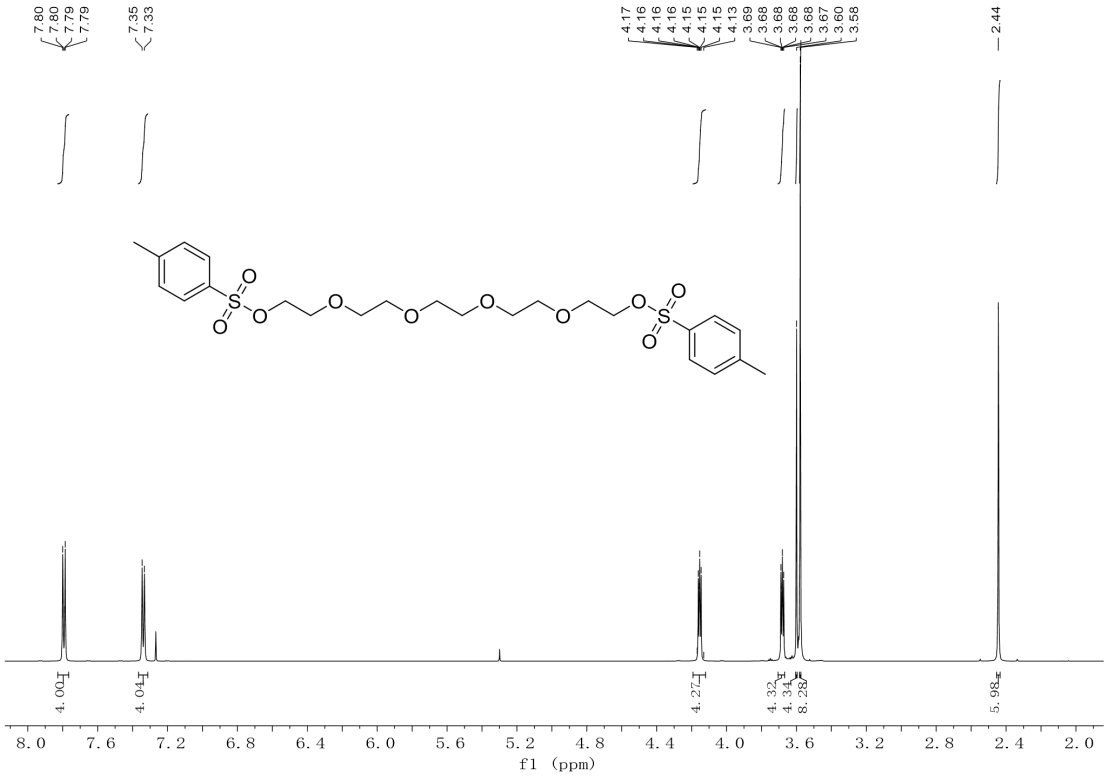

Supplementary Figure 1 ^{1}H NMR spectrum of compound **2** in $CDCl_3$ at 298 K.

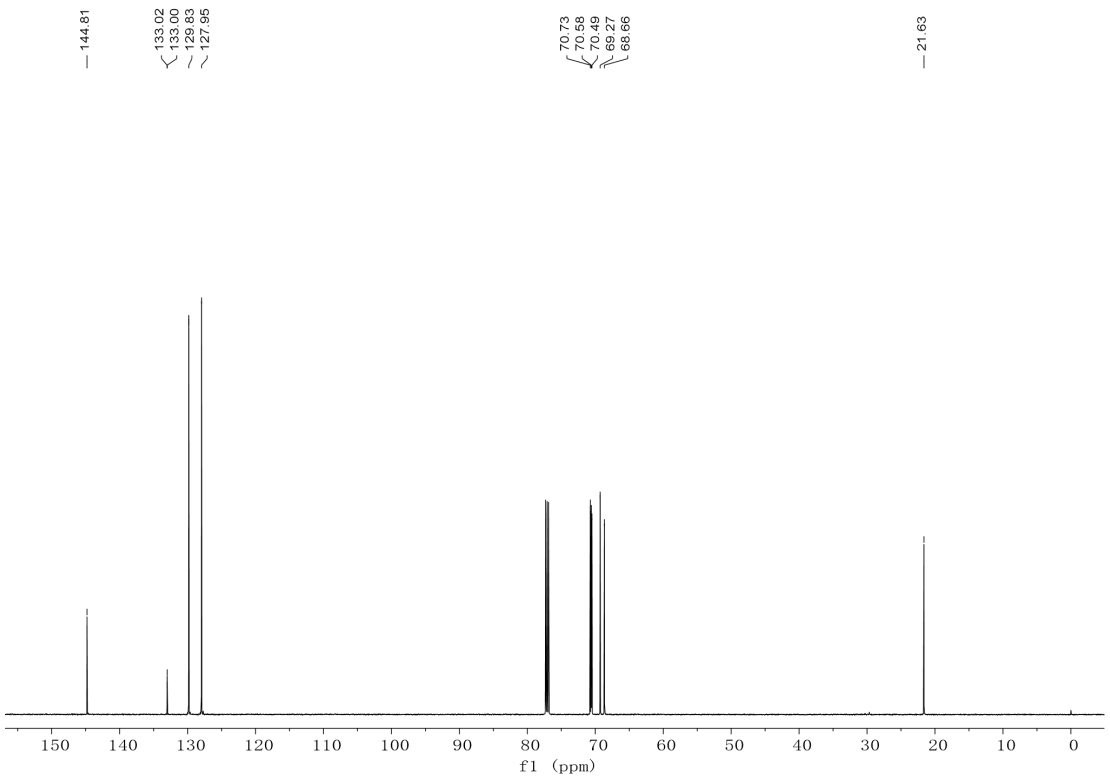

157

158 **Supplementary Figure 2** ^{13}C NMR spectra of compound **2** in $CDCl_3$ at 298 K.

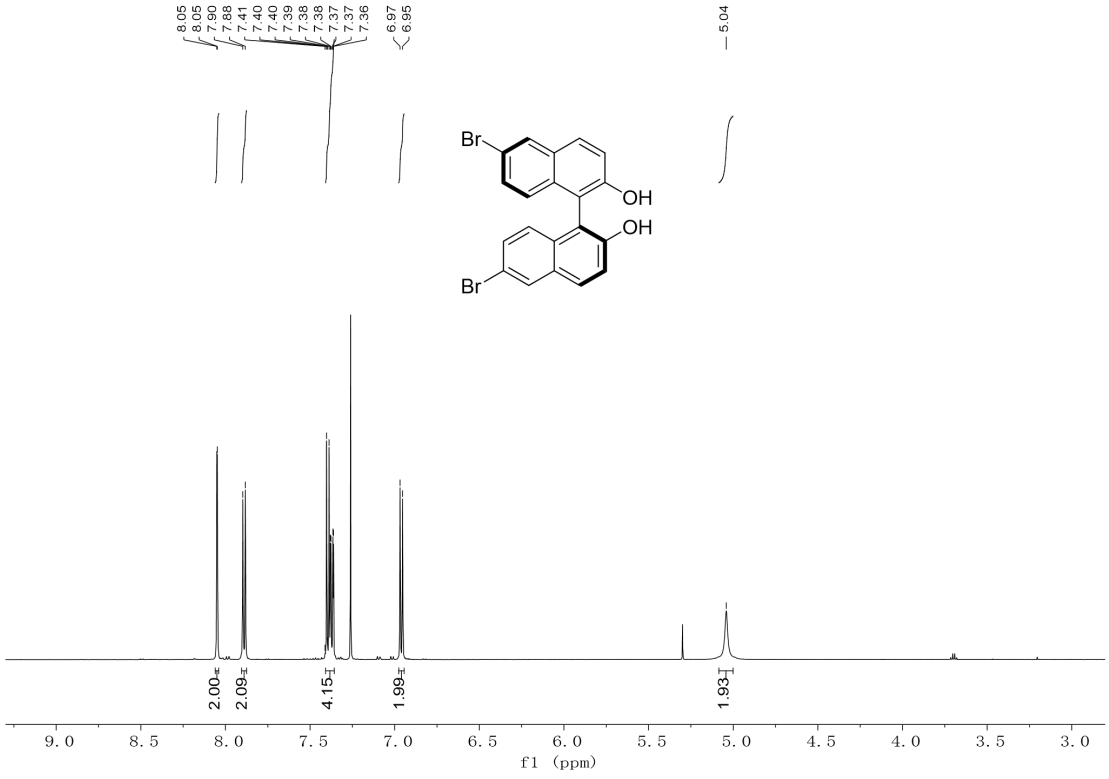

159

160 **Supplementary Figure 3** ^{1}H NMR spectrum of **(*S*)-4** in $CDCl_3$ at 298 K.

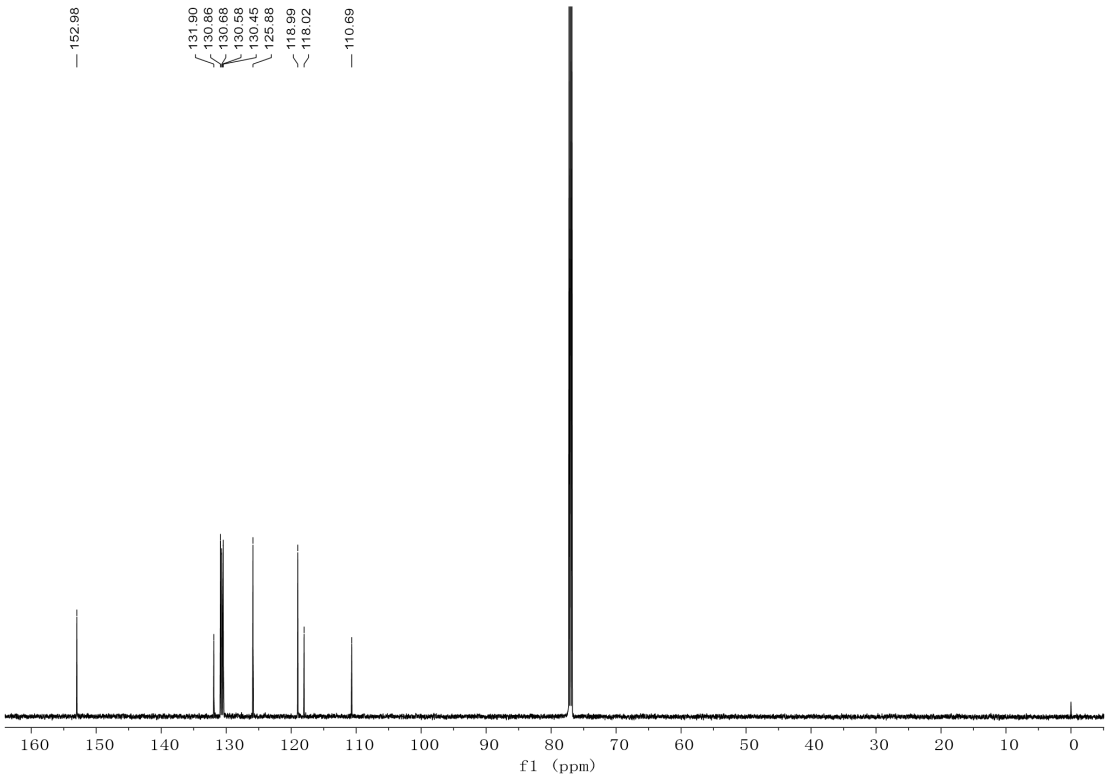

Supplementary Figure 4 ^{13}C NMR spectrum of **(*S*)-4** in $CDCl_3$ at 298 K.

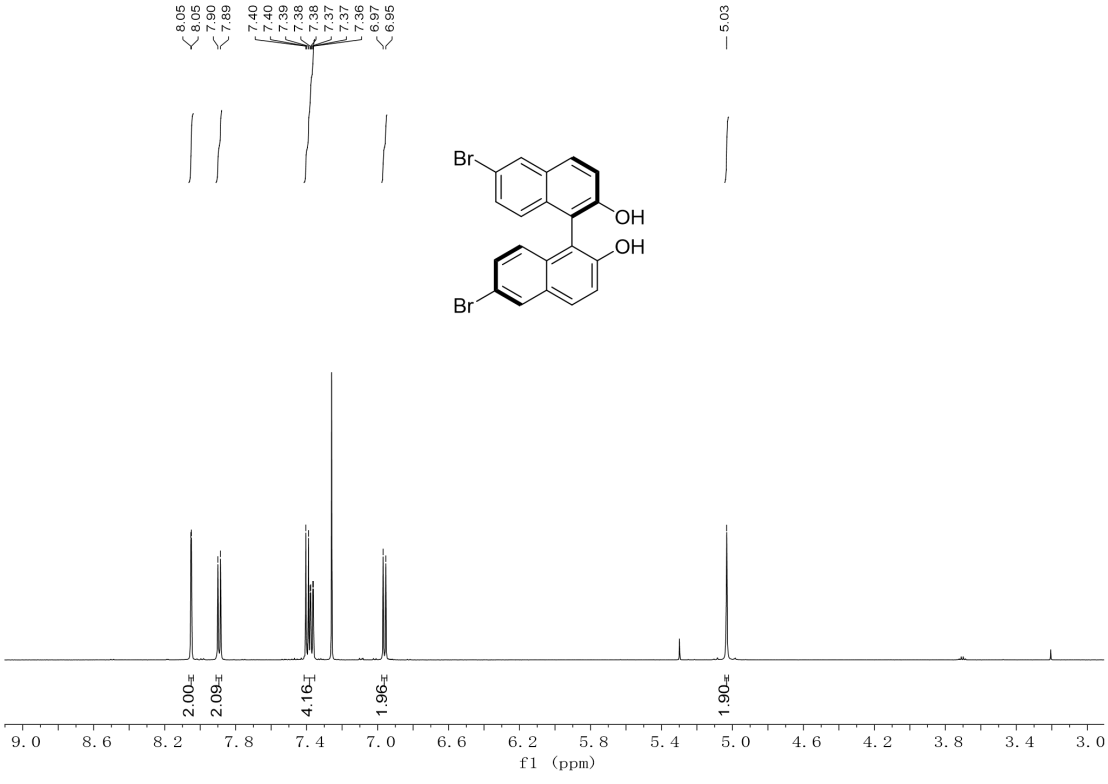

Supplementary Figure 5 ^{1}H NMR spectrum of **(*R*)-4** in $CDCl_3$ at 298 K.

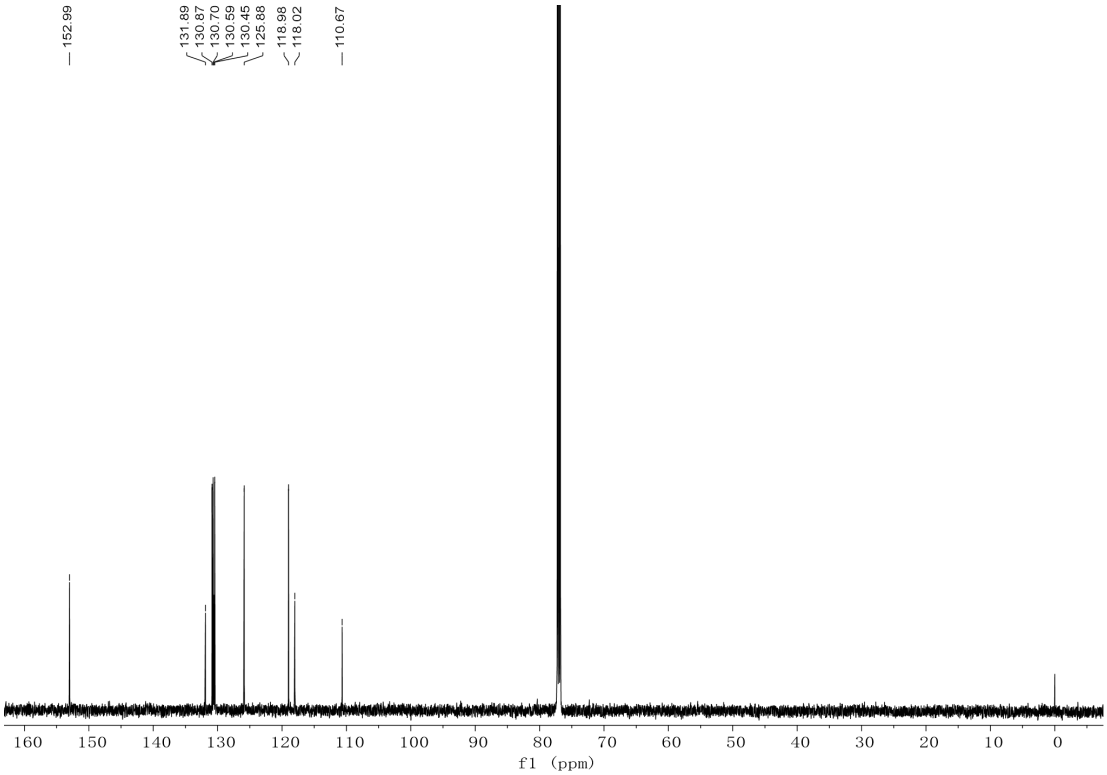

Supplementary Figure 6 ^{13}C NMR spectrum of **(*R*)-4** in $CDCl_3$ at 298 K.

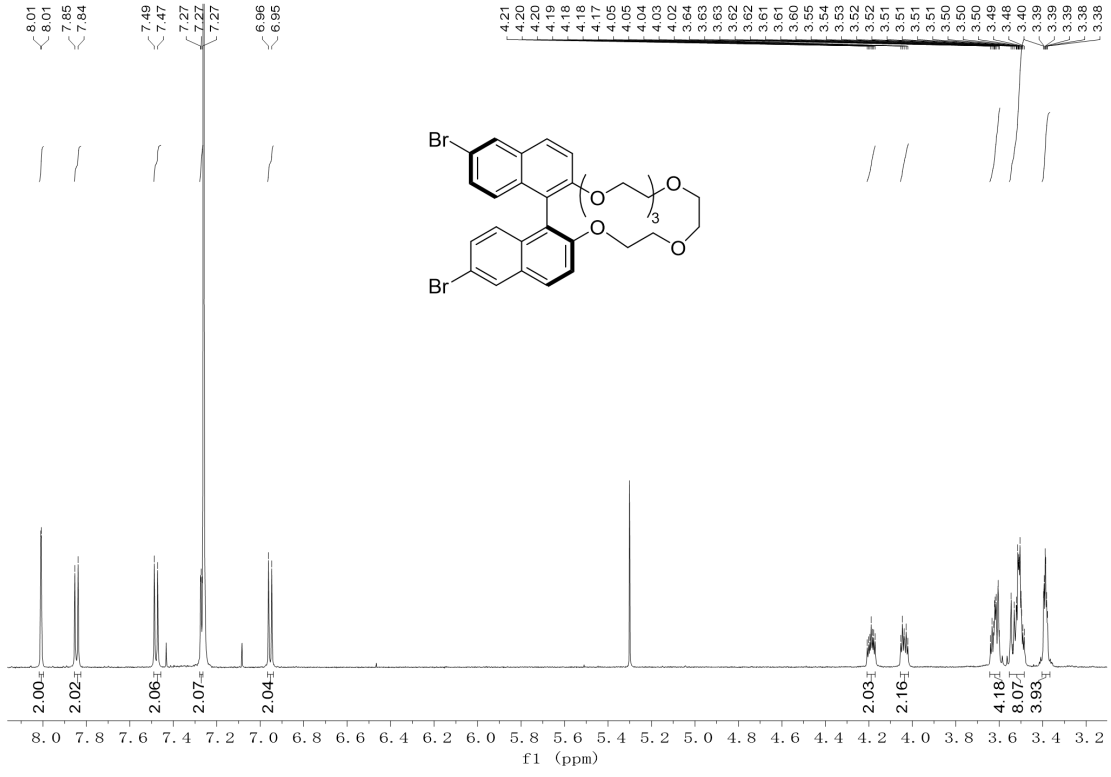

Supplementary Figure 7 ^{1}H NMR spectrum of **(*S*)-5** in $CDCl_3$ at 298 K.

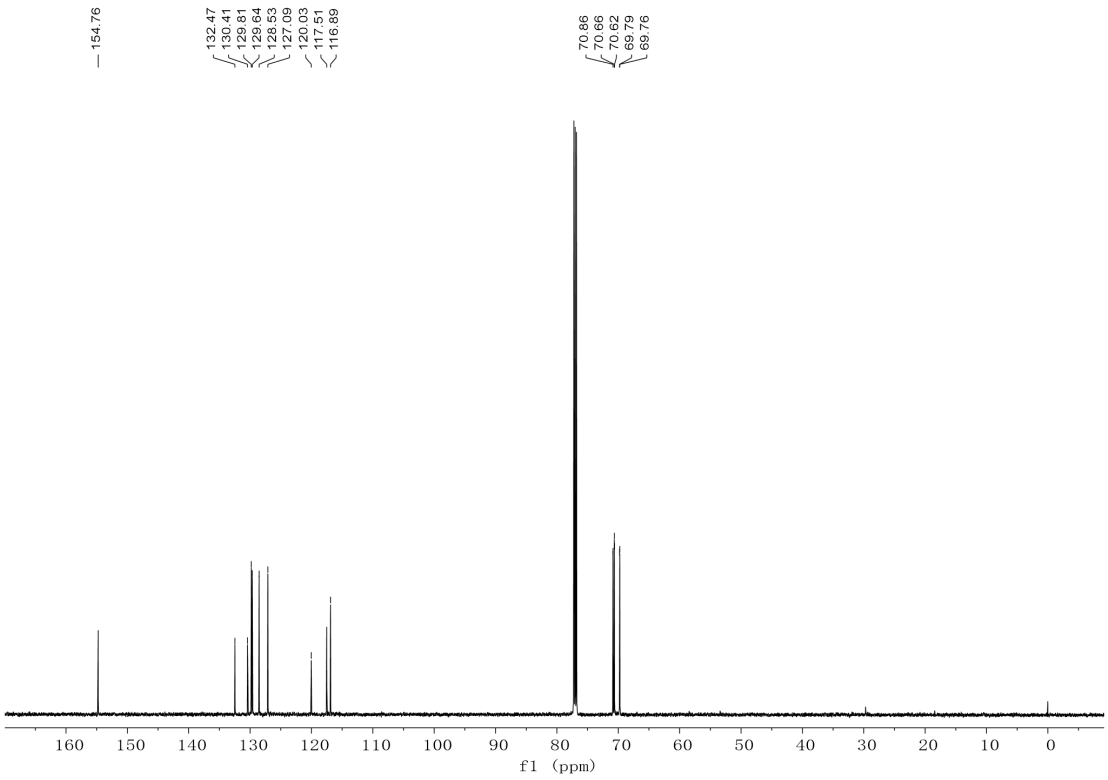

169

170 **Supplementary Figure 8** ^{13}C NMR spectrum of **(*S*)-5** in $CDCl_3$ at 298 K.

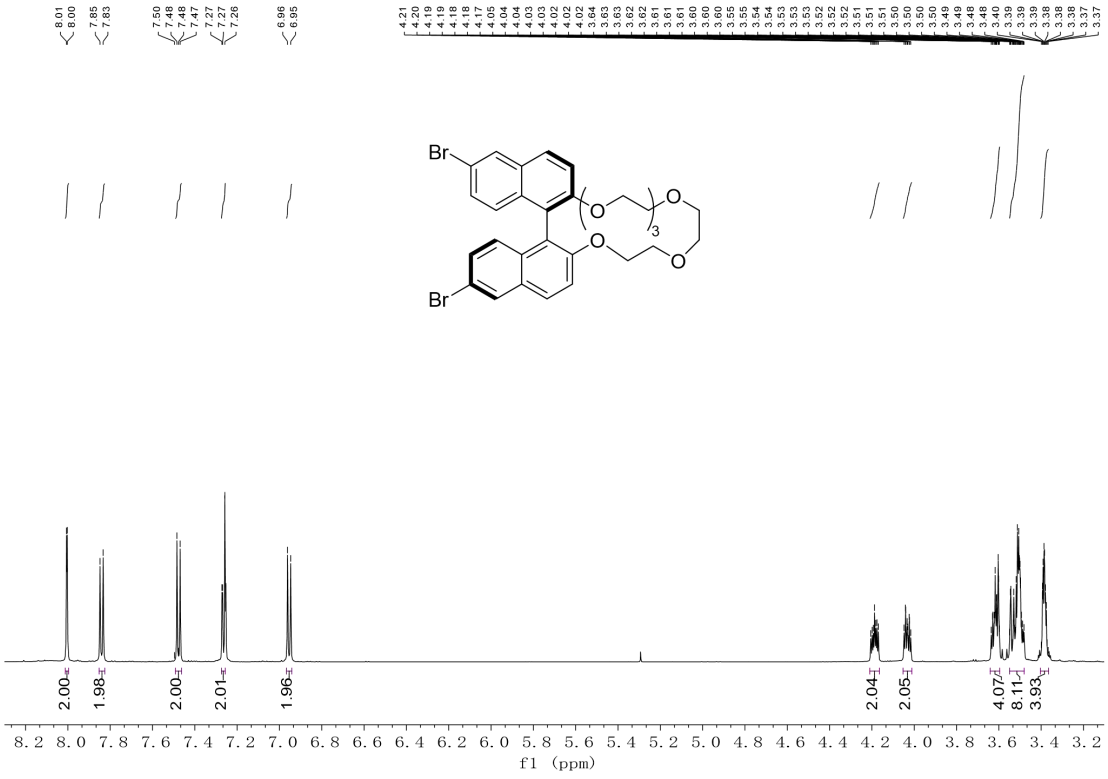

171

172 **Supplementary Figure 9** ^{1}H NMR spectrum of **(*R*)-5** in $CDCl_3$ at 298 K.

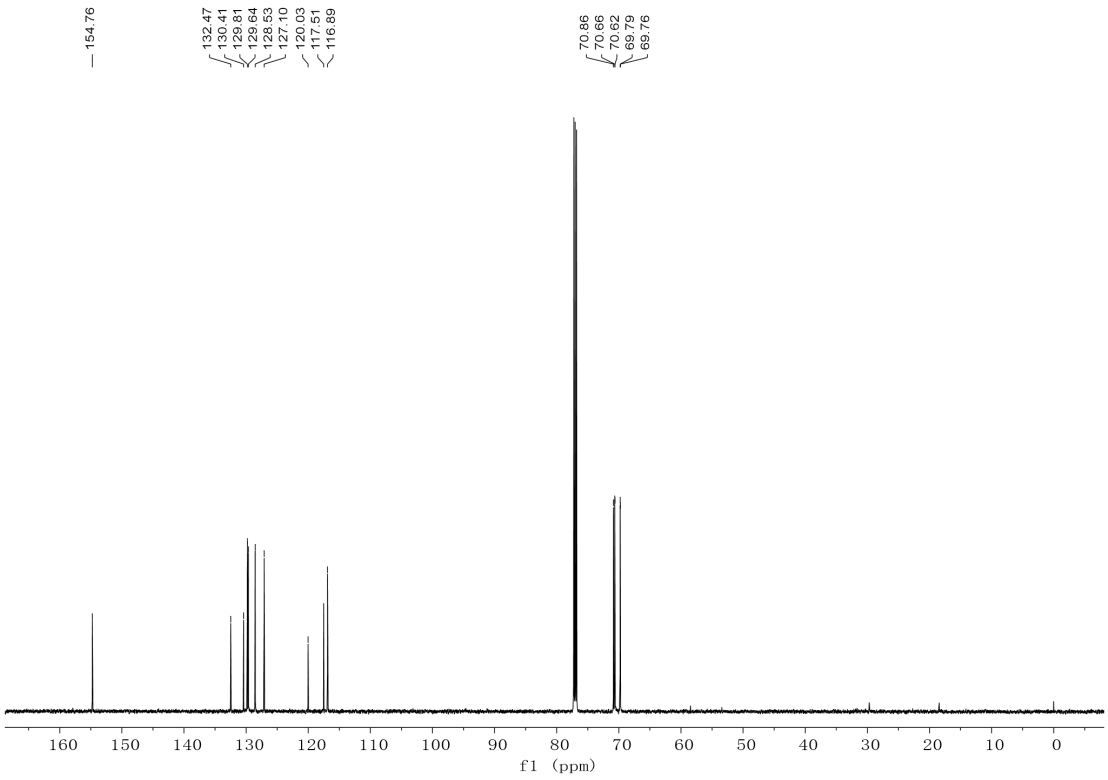

173

174 **Supplementary Figure 10** ^{13}C NMR spectrum of **(*R*)-5** in $CDCl_3$ at 298 K.

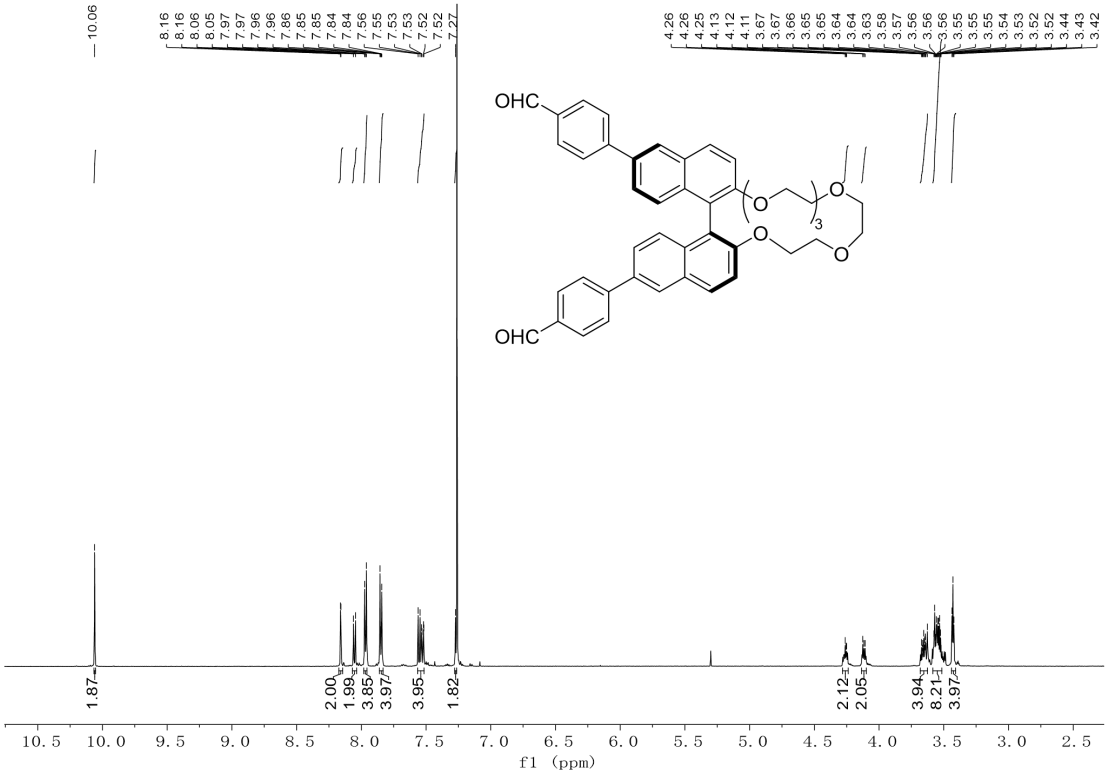

175

176 **Supplementary Figure 11** ^{1}H NMR spectrum of **(*S*)-7** in $CDCl_3$ at 298 K.

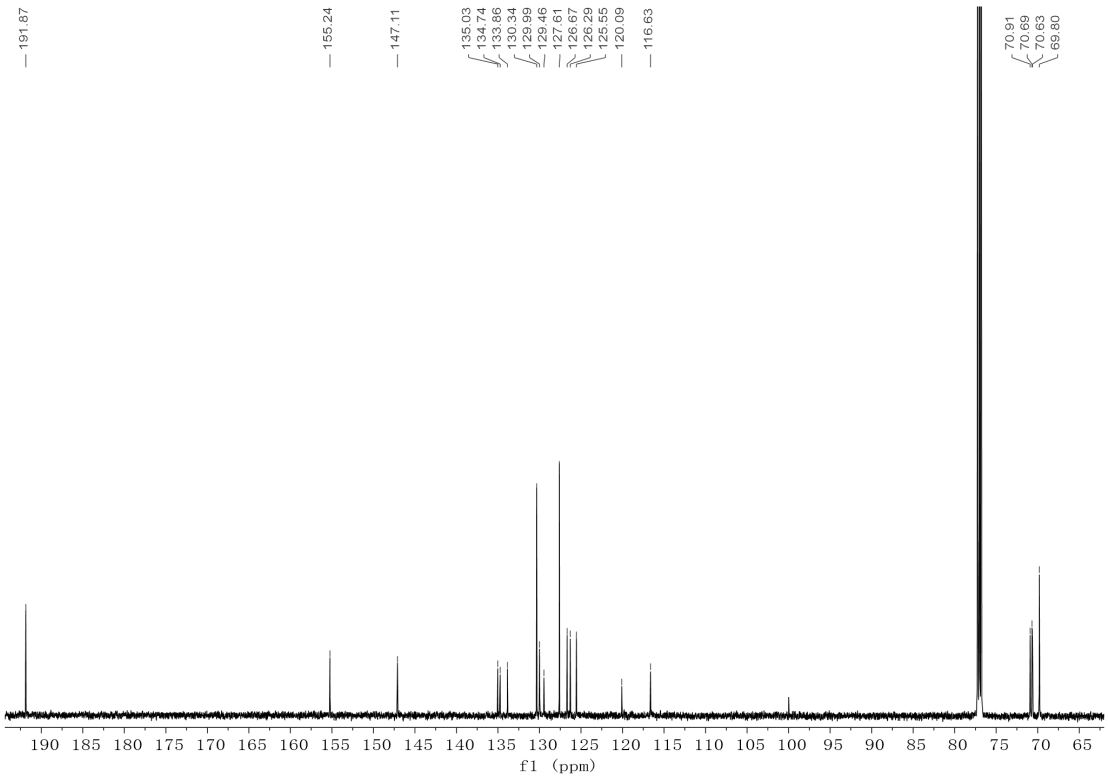

177

178 **Supplementary Figure 12** ^{13}C NMR spectrum of **(*S*)-7** in $CDCl_3$ at 298 K.

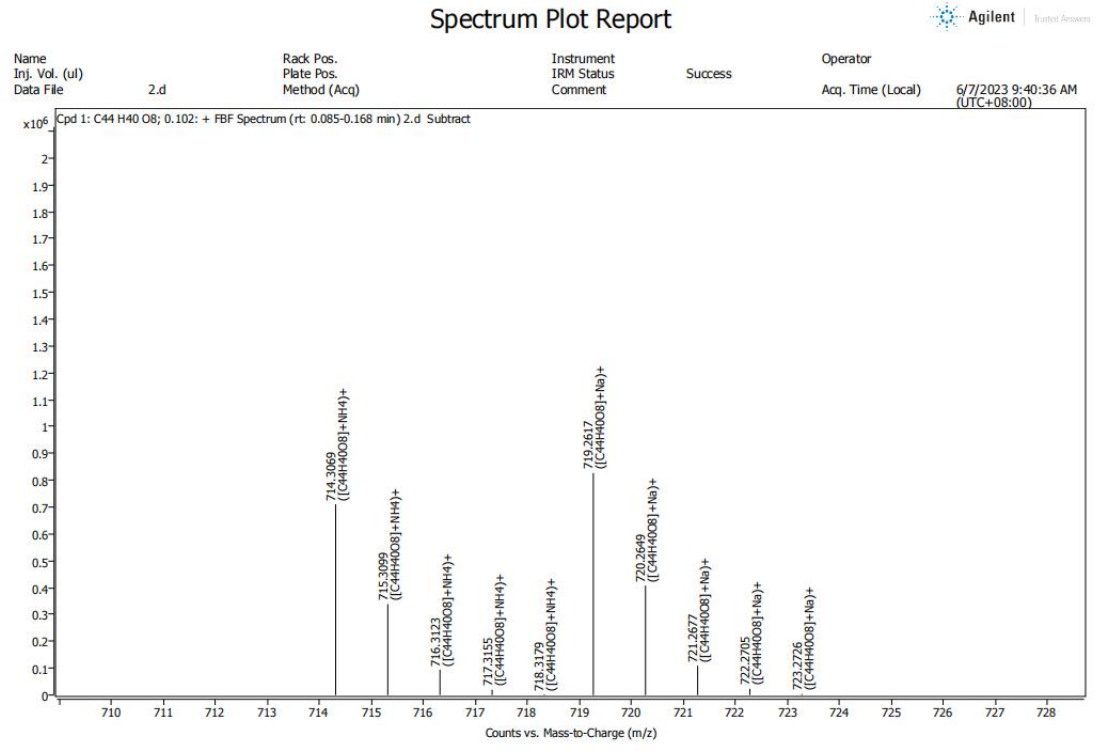

179

180 **Supplementary Figure 13** ESI-HRMS (Q-TOF) spectrum of **(*S*)-7**. ESI-HRMS

181 (Q-TOF) (*m/z*) Calcd. for $[$**(*S*)-7** + $NH_4]^+$:714.3067; Found: 714.3069. Calcd. for

182 $[$**(*S*)-7** + $Na]^+$: 719.2621; Found:719.2617.

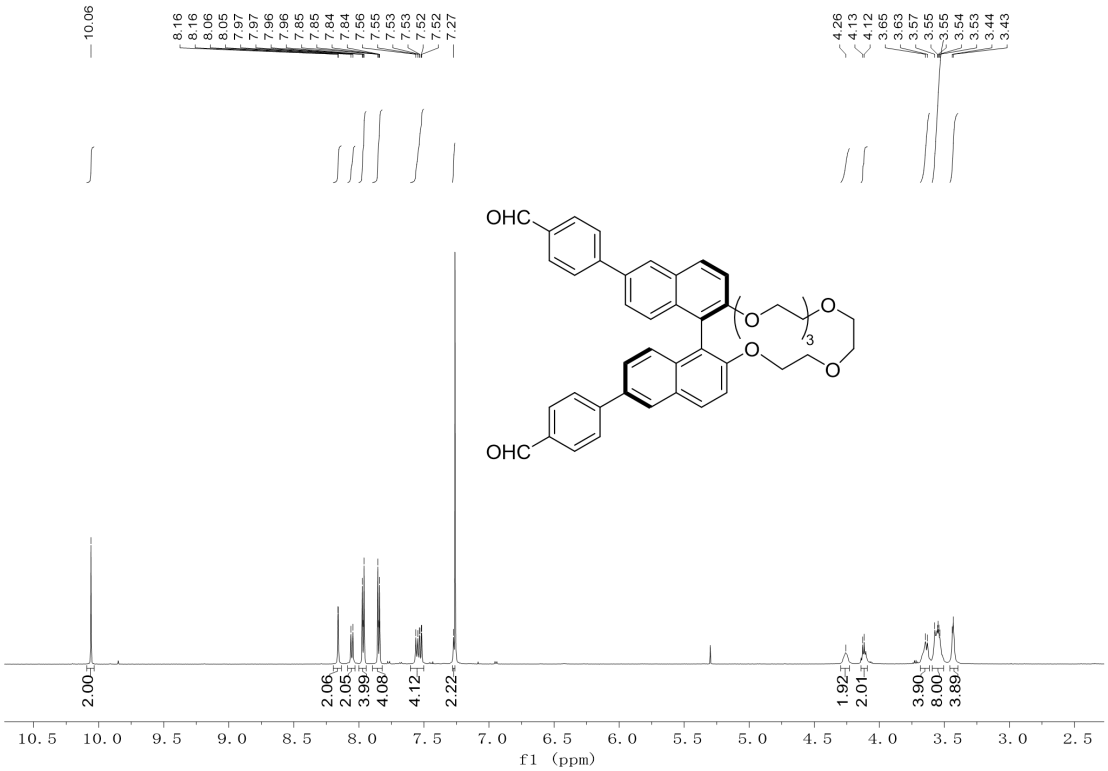

183

184 **Supplementary Figure 14** ^{1}H NMR spectrum of **(*R*)-7** in $CDCl_3$ at 298 K.

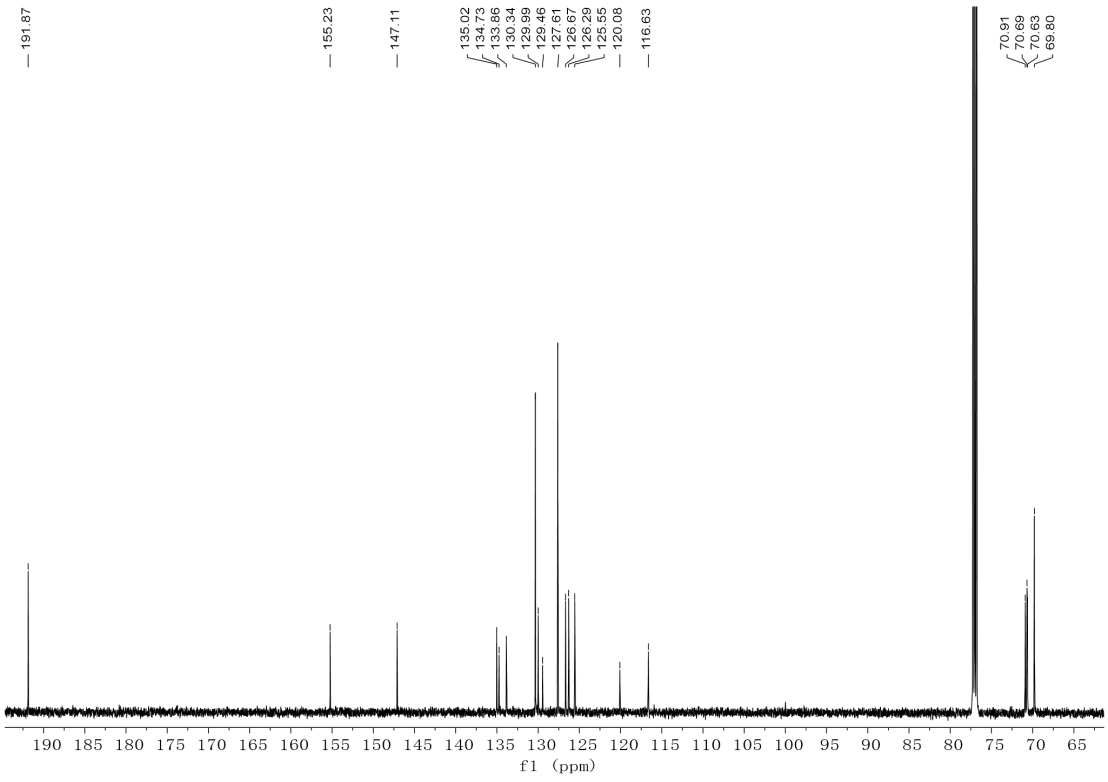

185

186 **Supplementary Figure 15** ^{13}C NMR spectrum of **(*R*)-7** in $CDCl_3$ at 298 K.

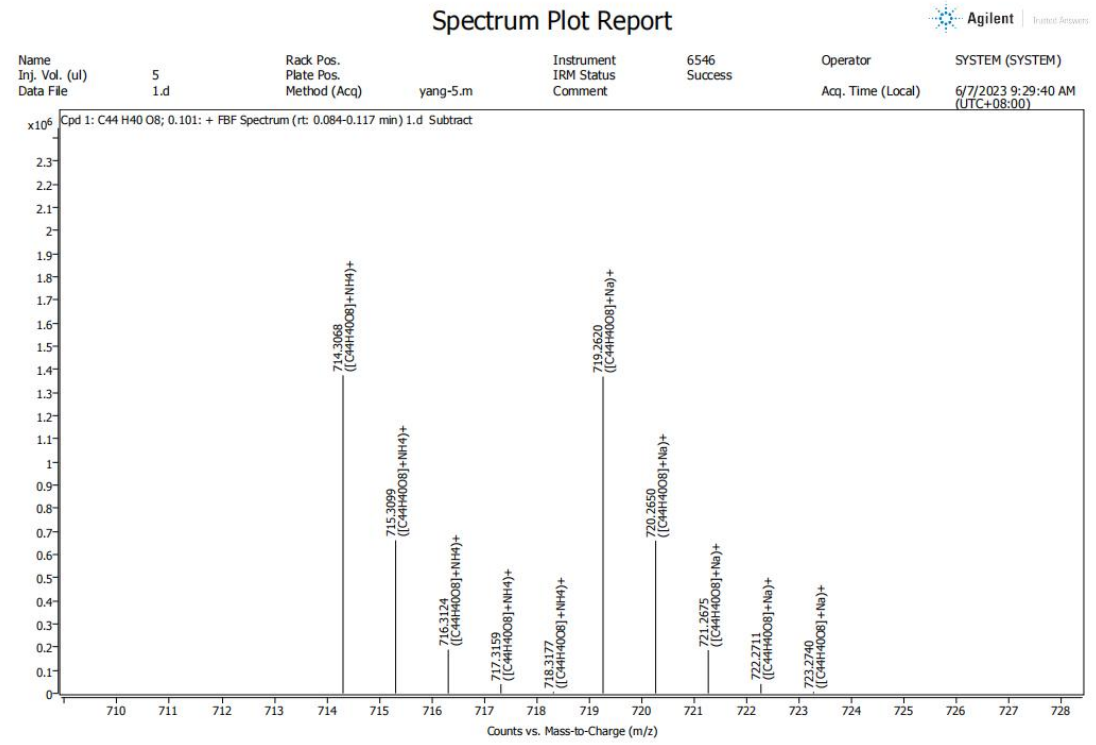

Supplementary Figure 16 ESI-HRMS (Q-TOF) spectrum of **(*R*)-7**. ESI-HRMS (Q-TOF) (*m/z*) Calcd. for [**(*R*)-7** + NH_4]$^+$:714.3067; Found: 714.3068. Calcd. for [**(*R*)-7** + Na]$^+$: 719.2621; Found:719.2620.

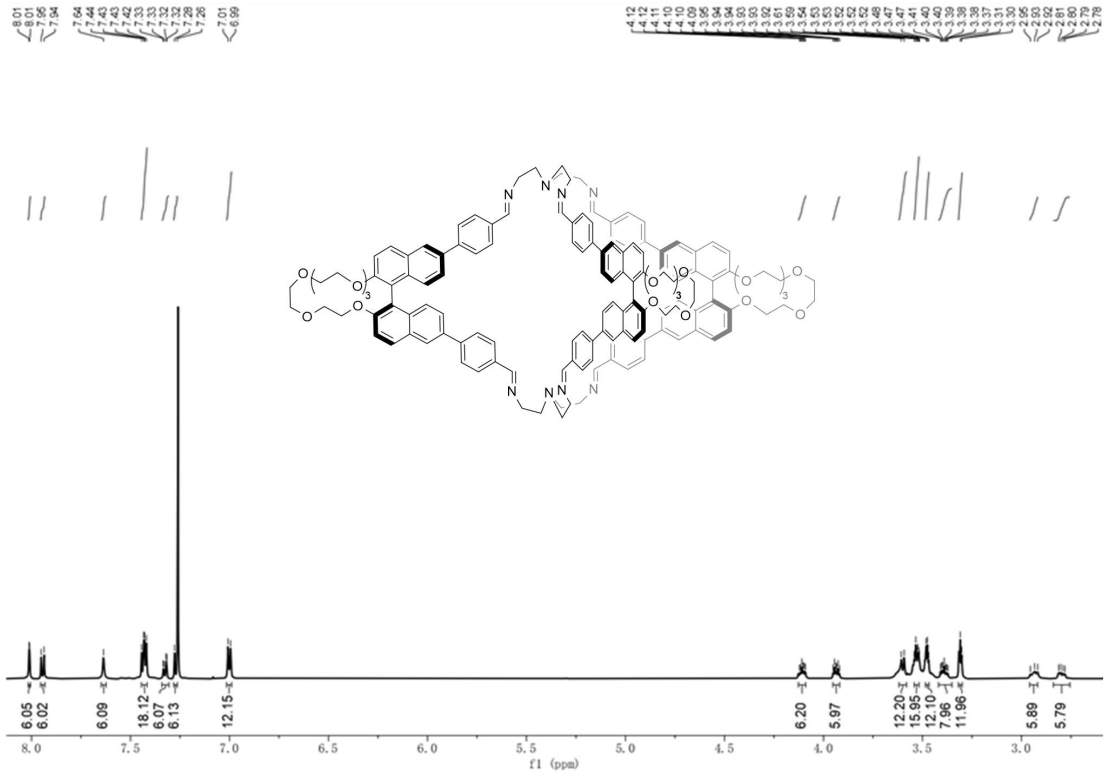

Supplementary Figure 17 ^{1}H NMR spectrum of **(*S*)-8** in $CDCl_3$ at 298 K.

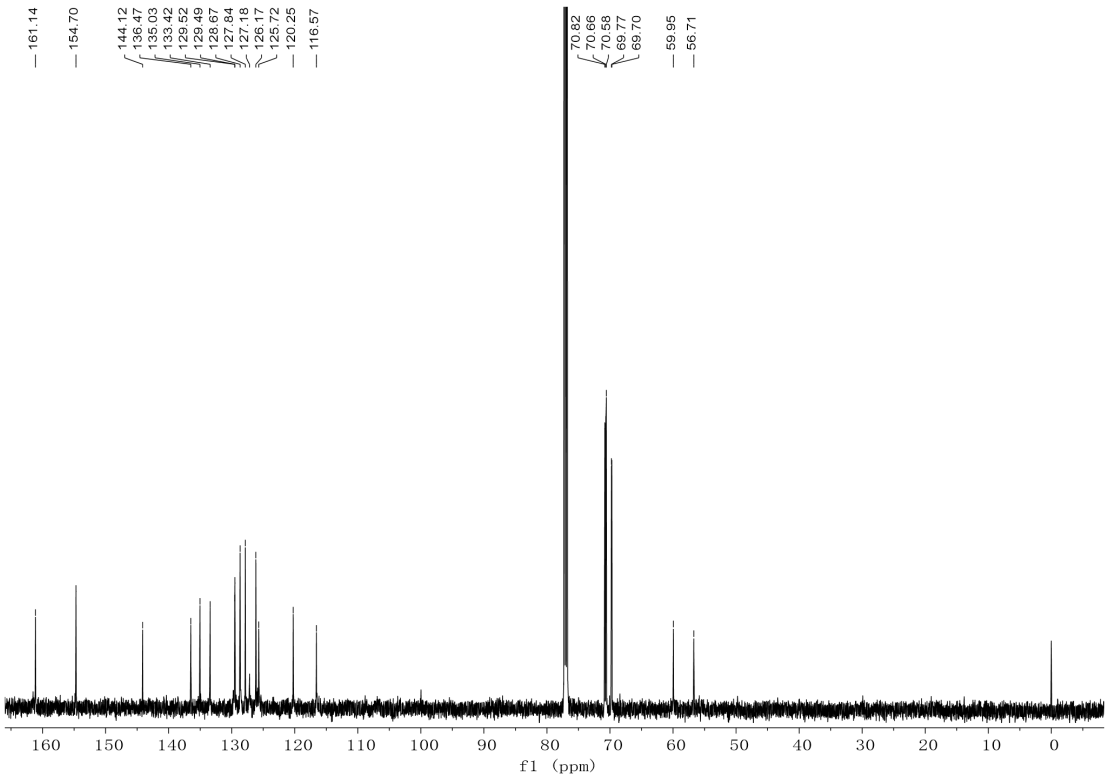

193

194 **Supplementary Figure 18** ^{13}C NMR spectrum of **(*S*)-8** in $CDCl_3$ at 298 K.

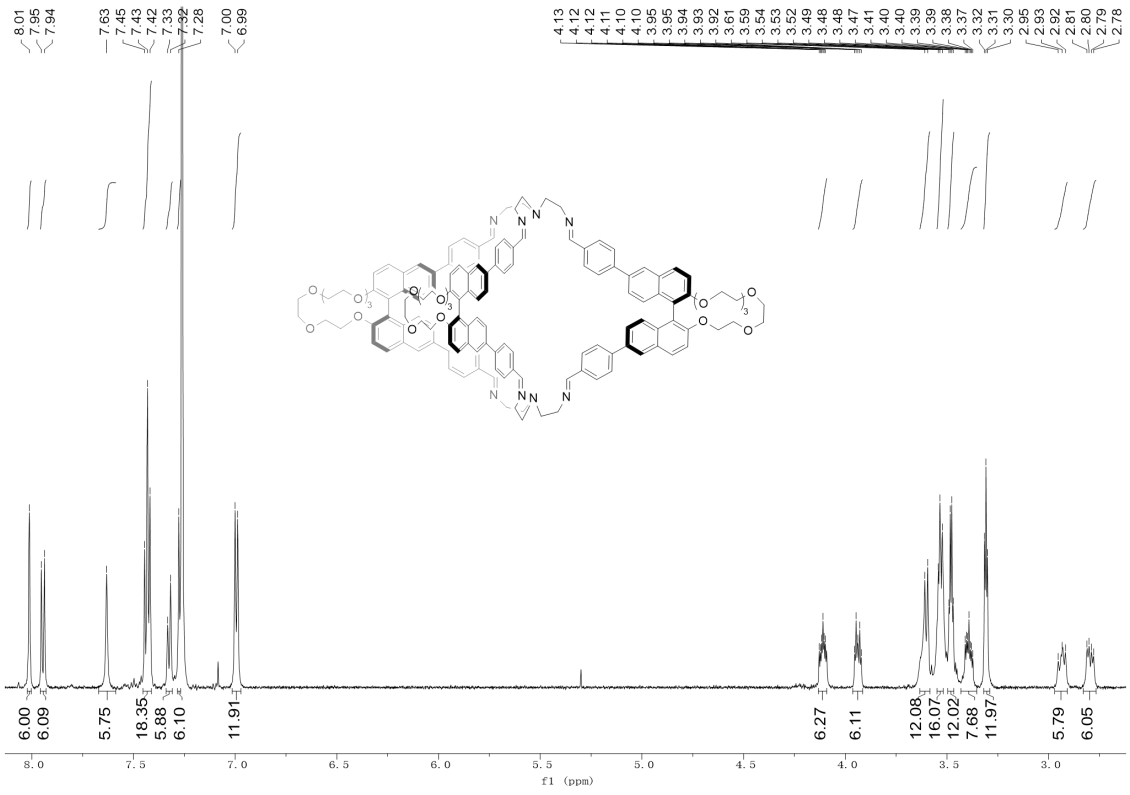

195

196 **Supplementary Figure 19** ^{1}H NMR spectrum of **(*R*)-8** in $CDCl_3$ at 298 K.

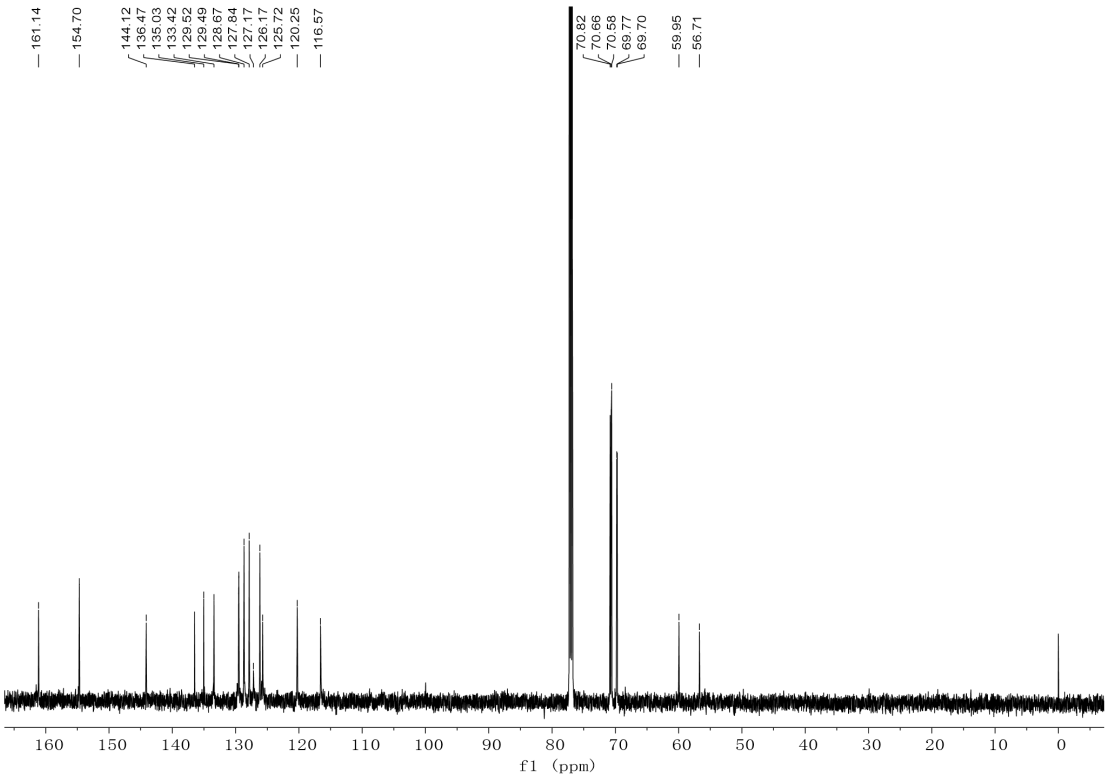

Supplementary Figure 20 ^{13}C NMR spectrum of **(*R*)-8** in $CDCl_3$ at 298 K.

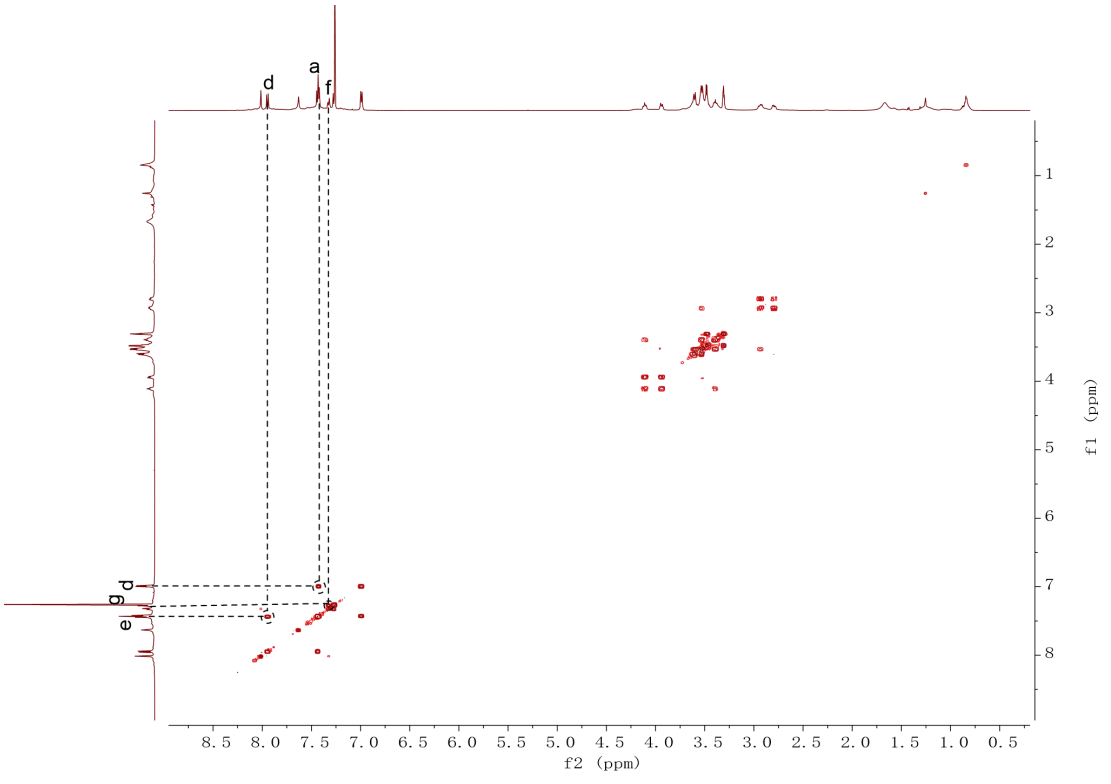

Supplementary Figure 21 ^{1}H-^{1}H COSY spectra of **(*S*)-8** in $CDCl_3$ at 298 K.

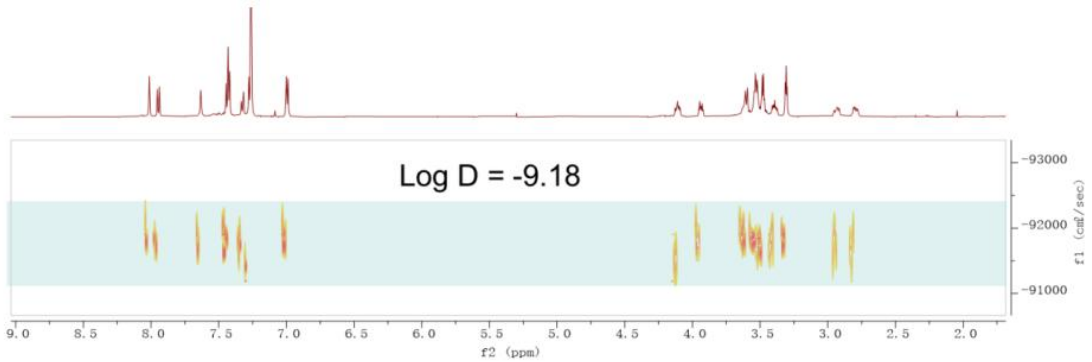

Supplementary Figure 22 DOSY spectrum of **(*S*)-8** in $CDCl_3$ at 298 K.

In Stokes-Einstein equation,

$$D = \frac{Tk_B}{6\pi\eta r}$$

which was applied to estimate the dynamic radius for the **Cage**. D is diffusion coefficient obtained from DOSY spectrum, kB is Boltzmann constant, T is temperature, Solvent viscosity η tested to be 0.57 mPa•s, and r is the estimated dynamic radius. The diffusion coefficient (D = 6.61 × 10^{-10} m^2/S) was also obtained, and the estimated dynamic radius (r = 11.6 Å) of cage could be calculated using the Stokes–Einstein equation.

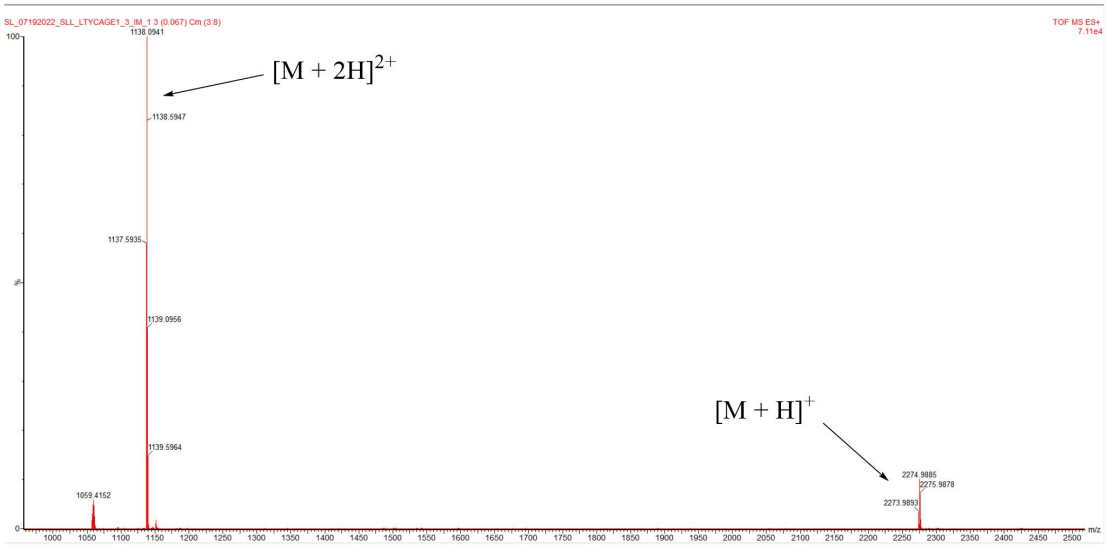

Supplementary Figure 23 ESI-MS spectrum of **(*S*)-8**. ESI-TOF-MS (*m/z*) Calcd. for $[M + H]^+$:2275.0676; Found: 2274.9885. Calcd. for $[M + 2H]^{2+}$: 1138.0941; Found:1138.0377.

2.7 Generation of the Molecular Model of Cage

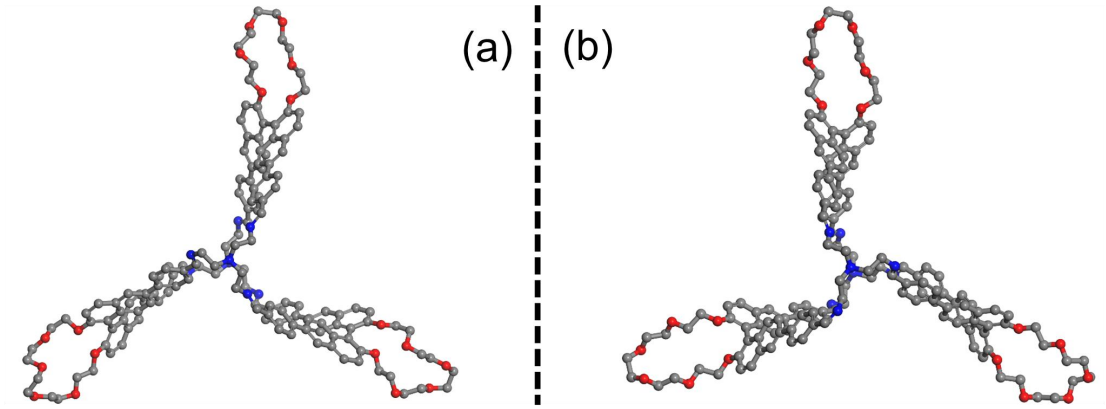

Supplementary Figure 24. The simulated crystal structures of **(*S*)-8** (a) and **(*R*)-8** (b). Energy-minimized molecular of **Cage** (N, blue; O, red; C, gray). Hydrogens are omitted for clarity. The specific methods are as follows: Firstly， compound **7** and tri(2-aminoethyl)amine were constructed in Materials Studio software and connected at appropriate angles. Then select tab Geomety Optimization by module Forcite in the software to optimize the structure of the cage.

3. Binding ratio, binding constant and limit of detection

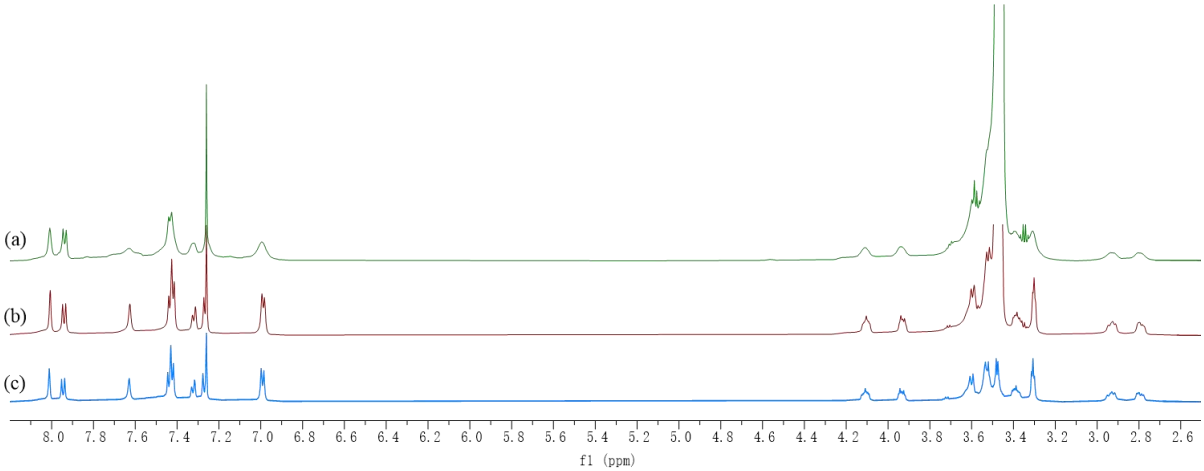

Supplementary Figure 25. ^{1}H NMR spectrum of **(*S*)-8** + 1 eq Hg^{2+} (a), **(*S*)-8** + 0.5 eq Hg^{2+} (b) and **(*S*)-8** (c) in CDCl3 at 298 K. $HgCl_2$ was dissolved in a small amount of diethyl ether (Trace amounts of diethyl ether could not cause any changes in ^{1}H NMR).

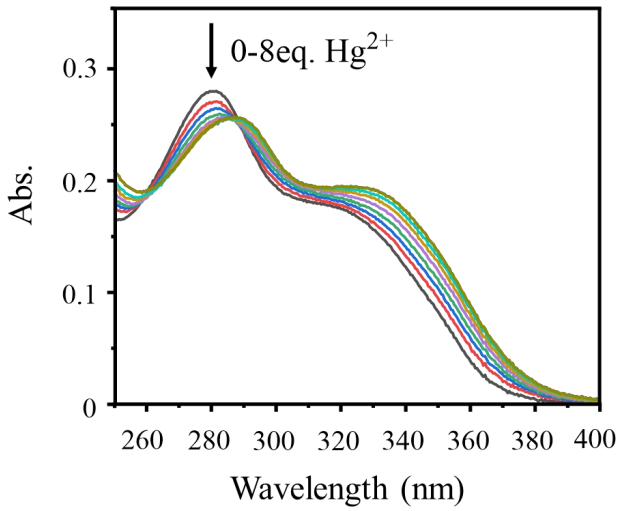

Supplementary Figure 26. Absorption spectra of cage after addition of Hg^{2+} up to 8 equiv.

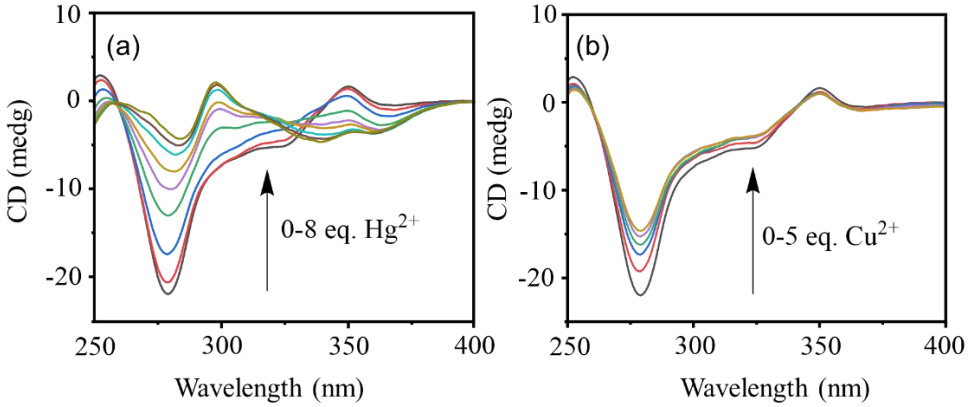

Supplementary Figure 27. CD spectral change with the equivalent of Hg^{2+} (a) and Cu^{2+} (b). According to the results, significant changes can be observed in Figure a, indicating that mercury ion can bind to the cage. There is no significant change in the Figure b, indicating that the cage cannot recognize copper ions.

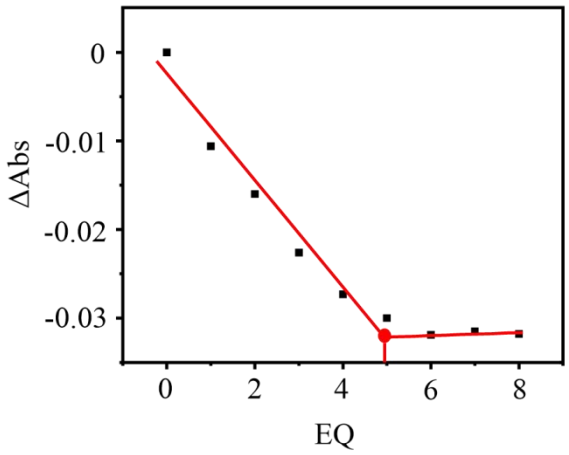

241

242 **Supplementary Figure 28.** Mole ratio plot of cage and Hg^{2+} (absorbance at 280 nm),

243 consistent with a 1:5 stoichiometry.

244

245

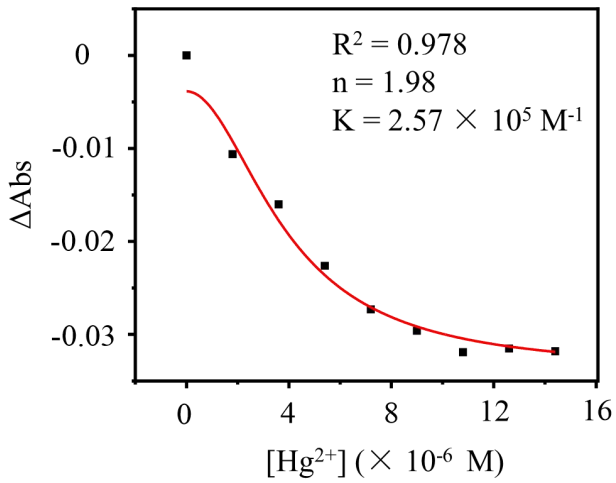

246

247 **Supplementary Figure 29.** Titration data with fitted curves of Hg^{2+} (absorbance at

248 280 nm) from Hill function[5].

249

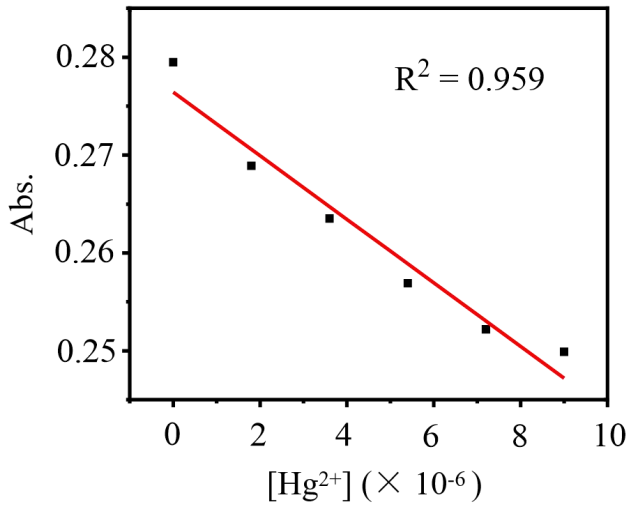

Supplementary Figure 30. The relationship between absorbance and Hg^{2+} concentrations (0-5eq.). The detection limit was calculated using the UV-vis titration data. In the absence of Hg^{2+} the UV-vis spectrum of a given receptor was recorded and the absorbance was measured ten times. The standard deviation of blank measurement was calculated. The detection limit was calculated using the following relation.

Detection limit = 3σ/K

Where, σ is the standard deviation of blank measurement and K is the slope between the absorbance versus Hg^{2+} concentration. According to the above formula, detection limit is 1.9×10^{-7} M.

4. The detection ability of cage at different pH

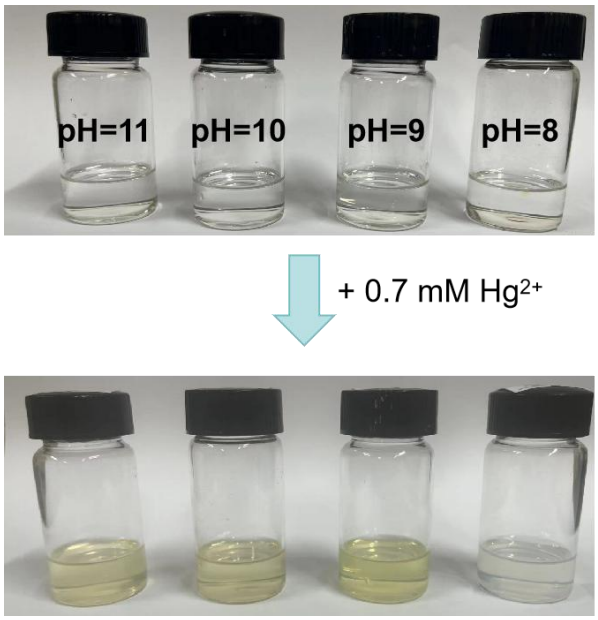

Supplementary Figure 31. Graphical illustration of Hg^{2+} ion detection at different pH. The concentration of cage was 0.2 mM.

5. Comparison table of mercury detection compared with some previously reported work

Supplementary Table 1. **Comparison table of mercury detection compared with some previously reported work**

probe	pH	LOD	method	Refs.
1	3-8	0.33 μg L^{-1}.	UV-vis	[6]
2	-	7.1×10^{-6} M	Fluorescence NMR UV-vis	[7]
3	-	0.718 ppm	UV-vis NMR	[8]
4	-	2.29 μM	Fluorescence	[9]
Cage	7-11	1.9×10^{-7} M	Naked eye Fluorescence NMR UV-vis	This work

6. References

1. Mao H, Thorne JB, Pharr JS, Gawley RE. Effect of crown ether ring size on binding and fluorescence response to saxitoxin in anthracylmethyl monoaza crown ether chemosensors. *Can J Chem* 2006;84:1273-9.[PMID:21562619 DOI:10.1139/v06-093 PMCID:PMC3090159]

2. Jones BA, Balan T, Jolliffe JD, Campbell CD, Smith MD. Practical and scalable kinetic resolution of BINOLs mediated by a chiral counterion. *Angew Chem Int Ed Engl* 2019;58:4596-600.[PMID:30779415 DOI:10.1002/anie.201814381 PMCID:PMC6492193]

3. Chakraborty C, Rana U, S. L. V. Narayana Y, Moriyama S, Higuchi M. Helical Fe(II)-based metallo-supramolecular polymers: effect of crown ether groups located

outside the helix on hydrous proton channel formation. *ACS Appl Polym Mater* 2020;2:4521-30. [DOI:10.1021/acsapm.0c00611]

4. Ramakrishna E, Tang JD, Tao JJ, et al. Self-assembly of chiral BINOL cages via imine condensation. *Chem Commun* 2021;57:9088-91.[DOI:10.1039/d1cc01507a]

5. Sheng TP, Fan XX, Zheng GZ, Dai FR, Chen ZN. Cooperative binding and stepwise encapsulation of drug molecules by sulfonylcalixarene-based metal-organic supercontainers. *Molecules* 2020;25:2656.[PMID:32521606 DOI:10.3390/molecules25112656 PMCID:PMC7321066]

6. Altunay N, Elik A, Demirbaş A, Kaya S, Maslov M. Investigations of Hg(II) analysis in real samples via computational chemistry, experimental design, and green microextraction approach. *J Food Compos Anal* 2021;102:104042. [DOI:10.1016/j.jfca.2021.104042]

7. Cao X, Zhao N, Gao A, Ding Q, Li Y, Chang X. Terminal molecular isomer-effect on supramolecular self-assembly system based on naphthalimide derivative and its sensing application for mercury(II) and iron(III) ions. *Langmuir* 2018;34:7404-15. [DOI:10.1021/acs.langmuir.8b00991]

8. Dar TA, Sankar M. Fused nickel(II) porphyrins-sensing of toxic anions and selected metal ions through supramolecular interactions. *Front Chem* 2020;8:595177. [PMID:33282838 DOI:10.3389/fchem.2020.595177 PMCID:PMC7705245]

9. Zhu H, Han C, Li Y, Cui G. Two new coordination polymers containing long flexible bis(benzimidazole) ligand as luminescent chemosensors for acetylacetone and Hg(II) ions detection. *J Solid State Chem* 2020;282:121132. [DOI:10.1016/j.jssc.2019.121132]